Received: 27 May 2020 | Revised: 6 August 2020 | Accepted: 30 August 2020

DOI: 10.1002/bit.27556

ARTICLE

BIOTECHNOLOGY AND BIOENGINEERING WILEY

Comparative investigation of fine bubble and macrobubble aeration on gas utility and biotransformation productivity

Benjamin Thomas[1] | Daniel Ohde[1] | Simon Matthes[2] | Claudia Engelmann[1] | Paul Bubenheim[1] | Koichi Terasaka[3] | Michael Schlüter[2] | Andreas Liese[1]

[1]Hamburg University of Technology, Institute of Technical Biocatalysis, Hamburg, Germany

[2]Hamburg University of Technology, Institute of Multiphase Flows, Hamburg, Germany

[3]Department of Applied Chemistry, Keio University, Yokohama, Japan

Correspondence

Andreas Liese, Hamburg University of Technology, Institute of Technical Biocatalysis, Denickestr. 15, 21073 Hamburg, Germany.
Email: liese@tuhh.de

Funding information

Deutsche Forschungsgemeinschaft, Grant/Award Numbers: LI 899/10-1, SCHL 617/14-1

Abstract

The sufficient provision of oxygen is mandatory for enzymatic oxidations in aqueous solution, however, in process optimization this still is a bottleneck that cannot be overcome with the established methods of macrobubble aeration. Providing higher mass transfer performance through microbubble aerators, inefficient aeration can be overcome or improved. Investigating the mass transport performance in a model protein solution, the microbubble aeration results in higher k_La values related to the applied airstream in comparison with macrobubble aeration. Comparing the aerators at identical k_La of 160 and 60 1/h, the microbubble aeration is resulting in 25 and 44 times enhanced gas utility compared with aeration with macrobubbles. To prove the feasibility of microbubbles in biocatalysis, the productivity of a glucose oxidase catalyzed biotransformation is compared with macrobubble aeration as well as the gas-saving potential. In contrast to the expectation that the same productivities are achieved at identically applied k_La, microbubble aeration increased the gluconic acid productivity by 32% and resulted in 41.6 times higher oxygen utilization. The observed advantages of microbubble aeration are based on the large volume-specific interfacial area combined with a prolonged residence time, which results in a high mass transfer performance, less enzyme deactivation by foam formation, and reduced gas consumption. This makes microbubble aerators favorable for application in biocatalysis.

KEYWORDS

aeration technology, gas utilization, glucose oxidase, microbubbles, multiphase reaction

Abbreviations: a, volume specific interfacial area (m^{-1}); c, concentration (mmol/L); c*, saturation concentration (mmol/L); d_{32}, Sauter mean diameter (mm); d_{av}, arithmetic mean diameter (mm); d_B, bubble diameter (mm); g, gravitational acceleration (m/s^2); H, Henry coefficient (mol/L*atm); k_L, liquid site mass transfer coefficient (m/s); k_La, volumetric mass transfer coefficient (1/s); p_{atm}, atmospheric pressure (kPa); T, temperature (°C); T, temperature (°C); U, enzyme activity (µmol/min); V_{Medium}, volume of reaction medium (L); vvm, liquid volume specific flow rate (min^{-1}); ρ, density (kg/m^3); σ, surface tension (mN/m); η, dynamic viscosity (mPa*s); τ, residence time (s); η_{EH}, gas utility enhancement factor (−); η_{op}, operative time efficiency factor (−); Δp, pressure difference (kPa); η_{O2} economy, oxygen atom economy (%).

1 | INTRODUCTION

To compare a novel fine bubble with classic macrobubble aeration techniques and prove the feasibility for application in biocatalysis, this contribution is focusing on oxygen as a gaseous substrate. Oxygen is by mass the third most abundant element in the universe and essential for a majority of life forms on earth. The air we are breathing is containing 0.21 vol.% oxygen (Weiss, 1970), which is a comparatively cheap and simply accessible natural source of oxygen for application in oxidation reactions (Toftgaard Pedersen et al., 2017). In industry, oxygen is employed as an oxidant in several applications from enzymatic oxidation reactions, biological aerobic wastewater treatment to whole-cell aerobic fermentation (Chapman, Cosgrove, Turner, Kapur, & Blacker, 2018; Hone & Kappe, 2018; Terasaka, Hirabayashi, Ai, Nishino, Fujioka, & Kobayashi, 2011). To make use of oxygen in enzymatic oxidation reactions, it has to be dissolved in a liquid phase to become accessible (Gemoets, Hessel, & Noël, 2016; Woodley, 2019). These reactions are often accompanied by mass transport limitations caused by the low oxygen solubility in aqueous media (Chapman et al., 2018; Garcia-Ochoa & Gomez, 2009). Therefore, the oxygen mass transfer performance of established aeration techniques are usually the bottleneck in process optimizations (Chapman et al., 2018; Romero, Gómez Castellanos, Gadda, Fraaije, & Mattevi, 2018). Considering this, there is a need for highly efficient aeration techniques in the industry. Requirements for these aeration systems are a high mass transfer performance, efficient gas utilization, low-pressure drop, low shear stress, and reduced foaming tendency (Terasaka, Hirabayashi, Nishino, Fujioka, & Kobayashi, 2011). One approach to achieve these goals is the cost-intensive application of pressure to enhance oxygen solubility in the system (Bolivar, Mannsberger, Thomsen, Tekautz, & Nidetzky, 2019; Xing et al., 2014). Another option is the bubble-free aeration through permeable or porous materials, which is challenged by the diffusion rate of oxygen through the membrane material (Kaufhold et al., 2012; Rissom, Schwarz-Linek, Vogel, Tishkov, & Kragl, 1997). A third possibility is aeration with fine bubbles, which are defined in the ISO 20480-1 to be a gaseous dispersed phase with a volume equivalent diameter of less than 100 µm (Tsuge, 2014). They are further differentiated in ultra-fine and microbubbles, which are less than 1 µm and between 1 µm and 100 µm of size, respectively. The generation of air containing fine bubbles through porous spargers, which are capable of generating microbubbles, are in the focus of this contribution. The mass transfer of fine bubbles as well as macrobubble aeration could further be enhanced by aeration with pure oxygen or enriched air (Lee, 2020; Lindeque & Woodley, 2020). Fine bubbles are successfully applied for the defouling of various surfaces, cleaning of sanitary facilities and in flotation processes (Tao, 2005; Wang, Wang, Yan, Wang, & Cao, 2017), and wastewater treatment (Wang et al., 2019; Khuntia, Majumder, & Ghosh, 2012; Temesgen, Bui, Han, Kim, & Park, 2017). The reported charged surface of small bubbles results in a lower coalescence, bursting tendency, and increased foam formation (Collins, Motarjemi, & Jameson, 1978; Huo et al., 2019; Oliveira & Rubio, 2011). In consequence, the introduced

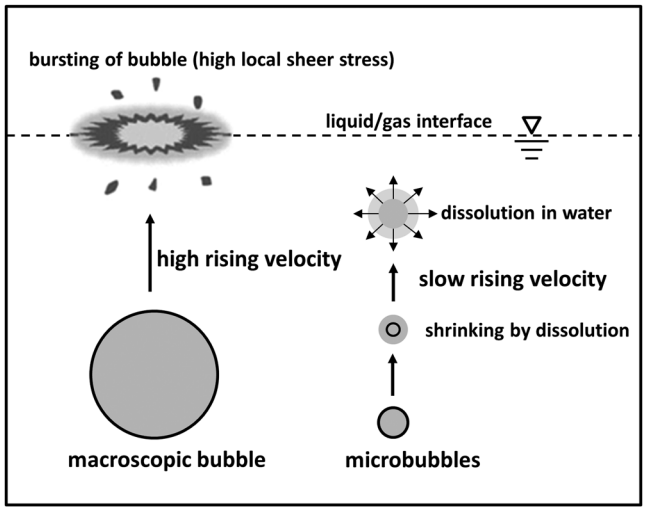

FIGURE 1 Schematic properties of macro- and microbubble behavior in solution

shear forces compared to macrobubbles are reduced as illustrated in Figure 1 (Duval, Adichtchev, Sirotkin, & Mermet, 2012; Ushikubo et al., 2010). Nevertheless, the application of microbubble instead of macrobubble aeration is known to reduce the foaming tendency as a result of high mass transfer and lower gassing rates (Tsuge, 2014). It seems that microbubbles completely dissolve in to the surrounding medium, which avoids or reduces the need for antifoaming agents (Guy, Carreau, & Paris, 1986; Jia, Xiao, & Kang, 2019).

Microbubble aeration offers several advantages due to its simple generation and promising high dissolution rates in aqueous media (Iwakiri et al., 2017; Jia et al., 2019). This enhanced mass transfer performance results first from the high volume-specific interfacial area and second from the prolonged residence time by low rising velocity as shown in Figure 1 (Duval et al., 2012; Struthwolf & Blanchard, 1984; Terasaka et al., 2011). Especially, the high interfacial area leads to the decrease in bubble size (shrinking) by quick dissolution, which is resulting in an exponential increase of the Young–Laplace pressure (inner bubble pressure), when the bubble size is decreased towards the microbubble region (Iwakiri et al., 2017). The bubble inner pressure is linked to the concentration gradient by the law of Henry (Atkins, de Paula, & Michael, 2013) in the boundary layer of the bubble. According to Henry's law, the partial pressure difference is the driving force for mass transferred from the bubble into the bulk phase which is the fundamental reason of fast shrinking and quick dissolution of microbubbles (Epstein & Plesset, 1950; Iwakiri et al., 2017; Ludwig & Macdonald, 2005). To make use out of these promising properties of microbubbles, the aeration has to be implemented in established reactor types, such as bubble column and stirred tank reactor (STR; B. Liu et al., 2019). The behavior of microbubbles is different compared with classic macrobubble aeration under stirrer induced shear forces, because of their lower volume, immobile bubble surface, and higher residence time (Liu, Zhang, Zhang, Yang, & Zhang, 2014; Struthwolf & Blanchard, 1984). For macrobubbles, the mass transfer performance is depending on the dispersion of the gaseous phase by agitation induced

shear forces (Gaddis, 2013; B. Liu et al., 2019). This is often coupled to high energy input, inefficient gas consumption, and waste of large amounts of gas (B. Liu et al., 2019; Terasaka et al., 2011). In consequence of the high gassing rates and energy input, macrobubble systems are simultaneously mixed extensively. In contrast, microbubbles have a low terminal rising velocity and provide, therefore, less efficient mixing induced by the applied gas stream (Parkinson, Sedev, Fornasiero, & Ralston, 2008). To ensure proper mixing conditions in microbubble aerated reactions, some agitation is needed. Thus, there is a potential to reduce the necessary energy input to a minimum.

For the investigation of microbubble application in biotransformation, an enzymatic model reaction system is studied in an aerated STR set-up. This study is focusing on the comparison of micro- and macrobubbles generated in an aerated STR (Figure 2).

To investigate the advantages of microbubble aeration techniques, the oxygen-limited biotransformation of β-D-glucose with oxygen towards gluconic acid and hydrogen peroxide catalyzed by glucose oxidase (GOx) from *Aspergillus niger* is chosen. The productivity (after 3.5 h), gas utilization, and mass transport performance of macro- and microbubble aeration are compared. To get a deeper understanding and interpretation of the effects influencing the productivity after 3.5 h, a detailed characterization of the model enzyme GOx Type VII from *A. niger* is carried out.

2 | MATERIAL AND METHODS

2.1 | Chemicals, enzymes and proteins

GOx from *A. niger* Type VII, peroxidase (POD) Type II from horseradish with 450 U/mg, catalase from the bovine liver with 5500 U/mg, and o-dianisidine more than or equal to 98% POD substrate were purchased from Sigma-Aldrich/Merck. The bovine serum albumin (BSA) was purchased from Carl Roth. The reaction media were composed of demineralized water, D(+)–glucose p.a. (Carl Roth), sodium acetate more than or equal to 99% (Sigma-Aldrich/Merck), acetic acid ROTIPURAN® 100% (Carl Roth), and sodium hydroxide more than or equal to 98% (Carl Roth).

2.2 | Devices

A UV/VIS photometer UvikonXL including temperature control was used in the activity assay. Incubation was carried out in a 500 ml glass reactor including a heating jacket connected to a Lauda 003 heating bath. The agitator was running with an IKA RW 20 digital overhead stirrer motor combined with the Bola pitch blade stirrer (45° blade) $d = 46$ mm. To ensure constant pH, the 848 Titrino plus Metrohm auto titration unit was included in the setup. The measurement of the oxygen concentration was performed with a Fibox 4 PreSens Precision Sensing GmbH using the oxygen sensor spot SP-PSt3-NAU-D5-YOP. The following aerators are tested in the aeration experiments: 1 µm pore size Shirasu Porous Glass (SPG) sparger frit from SPG Technology Co., Ltd., 2 µm pore size sinter stone from Techlab GmbH, open pipe with an opening diameter of 5 mm, and a 6-hole open pipe with openings of 0.5 mm. The flow rate was adjusted by a Hosco Unitec flow meter 0.4–5 N L/min and a Thermoflow from Profi Mess GmbH flow meter 4–200 ml/min. The surface tension was measured with the DVT50 drop volume tensiometer from Krüss. The bubble size distribution (BSD) was determined using the optical probe Sopat-VI Sc.

2.3 | Photometric activity assay

The determination of the initial enzyme activity was carried out based on the GOx/POD assay by Bateman and Evans. A substrate

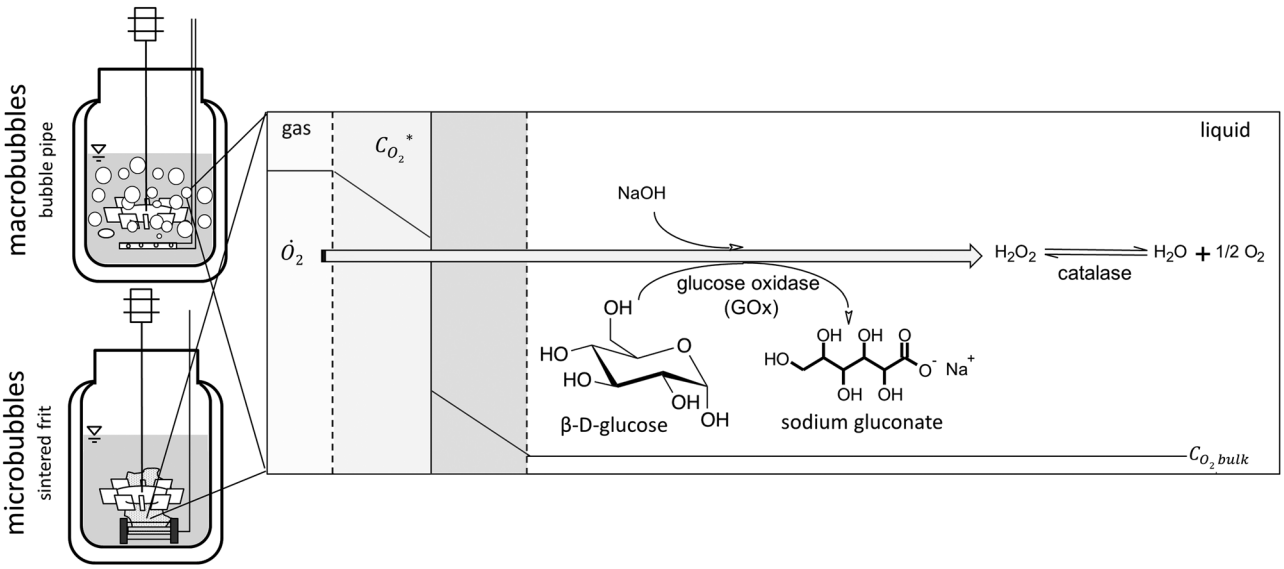

FIGURE 2 Concept of enzymatic sodium gluconate synthesis in a two-phase system. The boundary layer is indicated with dashed lines

solution containing 0.21 mM o-dianisidine and 9.44 mM D-glucose in 10 mM sodium acetate buffer pH 5.3 was prepared. The samples contained 936 µl substrate solution mixed with 32 µl POD solution (60 U/ml) and 32 µl GOx solution (40 U/ml). As reference measurement, a composition of 936 µl substrate solution, 32 µl POD solution (60 purpurogallin U/ml), which was filled up to 1 ml with 10 mM sodium acetate buffer pH 5.3 was measured. The assay was initiated by the addition of the GOx solution. According to Bateman and Evans, the unit definition is: one unit is oxidizing 1.0 µmole of β-D-glucose to D-gluconolactone and H_2O_2 per minute at pH 5.3 and 30°C, which is equivalent to an O_2 uptake of 22.4 µmol per min (Bateman & Evans, 1995).

2.4 | Determination of mass transfer performance (k_La)

The k_La measurements were performed in 1 L (liquid) medium at 25°C in a 2-L STR. To ensure turbulent flow regime Re ≥ 10^4, a pitched blade turbine with a power input of 0.12 W/L was installed. The following aerators were tested: 1 µm pore size SPG, 2 µm pore size sintered frit, and a 5-mm open pipe. For the measurements, a 1-L model solution composed of 0.22 M D(+) glucose, 83.3 mg/L BSA in 10 mM sodium acetate buffer was used. A flow meter was installed to adjust the flow rate in the range of 0.0067–16.66 vvm. The mass transfer performance was determined according to the dynamic method described by (Garcia-Ochoa & Gomez, 2009; Tribe, Briens, & Margaritis, 1995). This method uses nitrogen for degassing to deplete the medium of oxygen and air to reach the saturation concentration c*. During aeration, the change in oxygen concentration c_n is measured. Applying the following linearization in Equation (1) using the time difference $t_n - t_0$ between the oxygen measurements, the dynamic k_La was determined.

$$k_La = ln\left(\frac{c^* - c_n}{c^* - c_0}\right)/(t_n - t_0) \quad (1)$$

2.5 | Experiments in an STR

The reaction setup was composed of a 500 ml jacketed glass reactor including three baffles and a pitch blade stirrer. To reduce the use of expensive enzymes in the gluconic acid synthesis, a 500-ml geometric equal reactor to the 2 l reactor filled with 300 ml medium was used. In this reactor, a down pumping pitch blade stirrer (45° blade, d = 46 mm) was applied. The gassing rate was adjusted by a flow meter. The tested aerators were the open pipe, SPG, and sintered frit as shown above. The substrate solution was containing 0.22 M D-glucose in 10 mM sodium acetate buffer. A temperature of 35°C and 450 rpm (0.12 W/L) was adjusted. The reaction was initiated by the addition of 11,865 U of GOx and approximately 12,000 U of catalase to the reaction mixture. To ensure a constant pH and monitoring of the productivity of gluconic acid, an auto titration unit was included in the setup. The reaction progress was measured by pH-stat titration of gluconic acid towards sodium gluconate. For the biotransformation, a constant pH of 5.3 was ensured with the continuous titration of 1 M sodium hydroxide solution.

2.6 | Bubble size and surface tension measurement

An endoscopic optical probe with a detection range of 9–1200 µm was used for the determination of the BSD. Measurements were carried out in an aerated STR, containing 83.3 mg/L GOx in 10 mM sodium acetate buffer pH 5.3, at a constant power input of 0.12 W/L (pitch blade stirrer) and a temperature of 25°C. In addition, the surface tension of different ratios of glucose and gluconic acid was measured with a DVT50 drop volume tensiometer from Krüss at 35°C.

3 | RESULTS AND DISCUSSION

For the comparison of aeration systems in biocatalysis regarding their gas utility, productivity, and oxygen atom economy, a suitable model enzyme is required. Therefore, the β-D-GOx Type VII from *A. niger* with an oxygen consumption rate of 450 µmol/min/mg_{Enzyme} (specific activity of v_{max} = 450 U/mg_{Enzyme}) is chosen. According to Equation (1), a k_La value below 417 1/h per mg of GOx (c* = 0.215 mmol/L, pure water, 35°C, 0.3 L) has to be adjusted to overcome the mass transfer limitation of the biotransformation. Due to this, an aerator dependent investigation of macro- and microbubble aeration (fine bubble), by studying the potential to enhance or overcome mass transfer limitation on the example of a model reaction system in biocatalysis, is carried out. Simultaneously, optimal reaction conditions for the biotransformation have to be adjusted to avoid the interfering effects from stability, pH, type of buffer, and so forth on the aeration related effects. In the literature, a pH optimum of 5–6 in sodium acetate buffer for GOx from *A. niger* (Bankar, Bule, Singhal, & Ananthanarayan, 2009) is reported, which is in good agreement to the determined optimal pH range in this study. The temperature-dependent activity optimum is measured to be in the range of 30–60°C, which confirms the literature data (Bankar et al., 2009; Wilson & Turner, 1992). Based on the investigation of the storage stability, suitable half-life times of 64.23 ± 18.22 h and 29.48 ± 7.72 h within the range of 30–40°C are identified. Bankar et al. (2009) reported for *A. niger* GOx a lower half-life time of 30 min at 37°C. In the literature for GOx mutants from *A. niger*, higher half-life times of 58–141 h are reported, which is in accordance with the stability determined in this study (Mafra, Furlan, Badino, & Tardioli, 2015). Furthermore, the Michaelis–Menten kinetics of the conversion of β-D-glucose were determined and a K_m of 11.7 ± 1.1 mM and V_{max} of 474.6 ± 12.4 U/mg (35°C) is obtained. In literature, a K_m of 33 mM and V_{max} of 458 U/mg for GOx from *A. niger* is reported (Bankar et al., 2009; Mafra et al., 2015). To avoid the accumulation of hydrogen peroxide during the reaction, which would act as an inhibitor

and deactivator (Silva, Tomotani, & Vitolo, 2011; Tomotani, das Neves, & Vitolo, 2005), catalase is added for its decomposition (Bao, Furumoto, Yoshimoto, Fukunaga, & Nakao, 2003; Hernandez, Berenguer-Murcia, C. Rodrigues, & Fernandez-Lafuente, 2012; Zhang et al., 2019). This changes the overall reaction equation to glucose + 0.5 O_2 reacting to gluconic acid. Therefore, partial recycling of O_2 from H_2O_2 by catalase is achieved (Bolivar et al., 2019). Nakamura, Hayashi, and Koga (1976) report a K_m, O_2 of 0.18 mM for an older mutant of GOx from *A. niger* at 25°C in 0.05 M acetate buffer at pH 5.5. Based on the enzyme characterization, further experiments are performed at 35°C and pH 5.3 in 0.3 L medium containing 87.8 mM D-glucose with 11,865 U of GOx and equal active catalase. The chosen GOx concentration relates to a theoretical oxygen consumption rate of 5932.5 µmol/min (under consideration of oxygen recycling by catalase), which would require a theoretical k_La of 5518.6 1/h to avoid mass transfer limitation.

3.1 | Determination of aerator mass transfer performance in the BSA model protein solution

Besides improving the oxygen saturation concentration through increased system pressure (Bolivar et al., 2019; Woodley, 2019) or through additives such as silicone oil (Leung, Poncelet, & Neufeld, 1997; Zhai et al., 2020), the system-specific aerator characterization in view of the oxygen mass transfer rate is the key to increase reaction rates. In respect to the oxygen solubility of 0.213 mM (35°C) and the above named $K_{m,O2}$ of 0.18 mM of GOx from *A. niger* (Nakamura et al., 1976), the gluconic acid synthesis is challenged by the low solubility of oxygen in water (Woodley, 2019). To circumvent this limitation, the optimization of the oxygen transfer rate (OTR) is necessary. In Equation 2, the cases for an oxygen (O_2) consuming reaction given mass transfer limitation is expressed. Therefore, the relation of OTR (µmol/min) to maximum reaction rate (v_{max} in µmol/min/mg) is used:

$$\frac{\text{OTR}}{v_{max} \bullet mg_{enzyme}} \begin{cases} \geq 1 \rightarrow no O_2 \text{limitation} \\ < 1 \rightarrow O_2 \text{limitation} \end{cases} \quad (2)$$

To overcome the oxygen mass transfer limitation for the above described GOx reaction, the ratio of oxygen supply (OTR) to oxygen demand (v_{max}) needs to be equal or higher than 1. In consequence, the enhancement of OTR in gluconic acid synthesis is essential to ensure high reaction rates. In respect to this and Equation (1), the OTR is directly linked to the volumetric mass transfer coefficient (k_La), which is a measure for mass transfer performance for the comparison of different aerator systems.

$$OTR = k_La(c^*\text{-}c^n)V_{Medium} \quad (3)$$

For improving the mass transfer performance in the model biocatalytic reaction, two microbubble aerators: a 2-µm sintered frit and a 1-µm SPG as well as two macrobubble aerators: single hole 5 mm open pipe and 6 × 0.5 mm open pipe are investigated and compared. According to Mersmann, the behavior of bubble deformation and generation is described by Weber (We) and Froude (Fr) number. The We is defined as the ratio of drag force (inertia force) to cohesion force and the Fr describe the relation of the flow inertia force to the gravity force (Mersmann, 1977; Räbiger et al., 2013). Especially the combination of high Young–Laplace pressure, immobile bubble surface (We/Fr < 0.3) and high volume-specific surface area of microbubbles is compared with classic macrobubble aeration. In contrast to microbubbles, macrobubbles show low self-compression (Young–Laplace pressure), mobile bubble surface (instabile primary bubbles), and low volume to surface ratio to investigate the effect of bubble size in enzymatic catalyzed model reactions (Mersmann, 1977; Räbiger et al., 2013). The microbubble aerators in this comparison are composed of porous materials with inhomogeneous pore size distributions. As reported in the literature, especially the pore size distribution is expected to affect the oxygen transfer rate through the generated bubbles size distribution (Kazakis, Mouza, & Paras, 2008b; Kulkarni & Joshi, 2005; Tsuge and Hibino, 1983). In previous investigations using the same microbubble aerators, no significant difference in the BSD between the SPG and sintered frit for gassing rates up to 0.067 vvm, generated in BSA containing sodium acetate buffer, is determined (Matthes et al., 2020). The 5 mm (single hole) open pipe macrobubble aerator and the 6 × 0.5 mm (multiple holes) open pipe are included in this comparison. Both the 5 mm open pipe and the 6 × 0.5 mm open pipe having a We of >> 2 and a We of >> 6 under the investigated flow rates and k_La values. This is proving that aeration in the jet gassing range is present for both macrobubble aerators, when using them to achieve a k_La of 160 and 60 1/h, respectively. In addition, the critical criteria for We^2/Fr >> 675, which is the critical ratio of secondary bubble formation, is fulfilled. Therefore, the correlation from Mersmann (1977) for both macrobubble aerators is applicable. According to this, large Weber numbers indicate that the impulse of gassing is high. In this case, instable primary bubbles formed at the aerator. These instable primary bubbles disintegrate shortly after generation and result in a secondary bubble formation. Out of the force balance, maximum stable bubble size is calculated, which is under the described applied gas stream, and Weber number a function of the liquid properties (Mersmann, 1977). Furthermore, a generated bubble is instable according to Mersmann for ratios of We/Fr ≥ 10. This condition is fulfilled in the case of both macrobubble aerators (5 mm open pipe and 6-hole open pipe [0.5 mm]). In consequence, the resulting Sauter mean diameter is independent of the size of the open pipe hole in the underlying study using 0.5–5 mm in this setup. Therefore, even the use of smaller multiple capillaries of 0.5 mm would theoretically result in the same Sauter mean diameter. However, this theoretical calculation is only applicable in pure water and neglects the introduced power input by stirring. Thus, deviation in the bubble size is expected, when using protein-containing solutions in an STR set-up (Durst & Beer, 1969; Mersmann, 1977; Räbiger et al., 2013). For example, the addition of the protein BSA is found to shift the BSD towards the microbubble

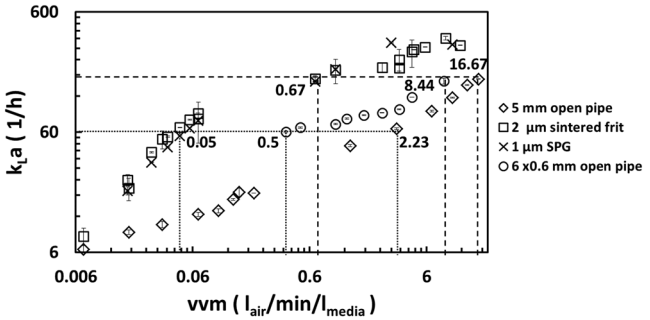

FIGURE 3 Comparison of the oxygen mass transfer performance depending on the inlet airflow and the aeration type (dynamic k_La determination with O_2 PreSens Fibox 4, reaction conditions: T = 25°C, V_{medium} = 1000 ml, 10 mM sodium acetate buffer pH 5.3, 87.8 mM D-glucose, 83.3 mg/L BSA, pitched blade turbine 430 rpm). BSA, bovine serum albumin; SPG, Shirasu Porous Glass

region. This effect is also expected for the application of GOx. The presence of glucose shows no significant influence on BSD (Matthes et al., 2020). To gain a deeper understanding of the aerator's specific mass transfer performance, the investigated range of aeration rate is expanded up to 16.667 vvm (Figure 3) from the previously studied lower aeration rates of up to 0.067 vvm (Matthes et al., 2020). Enabling the comparison of the aerators by mass transfer phenomena in the underlying study, the GOx is substituted by BSA to ensure the steady-state condition and avoiding an overestimation of the k_La through the consuming GOx reaction (Figure 3). In this study, it is assumed that BSA and GOx behave similarly on the liquid properties and multiphase flow. In respect to this, the aerators are characterized in a model reaction solution containing BSA protein and D-glucose in sodium acetate buffer (Figure 3).

In the evaluation of the microbubble aerators, the k_La performances of SPG and sintered frit are resulting in a similar characteristic (Figure 3). In contrast to the macrobubble aeration (5 mm open pipe, 6 × 0.5 mm open pipe), both microbubble aerators show a significantly higher mass transfer as shown in Figure 3. One reason for the observed behavior is the generation of fine bubbles, which are detected in BSD measurements (Figure 5). Both macrobubble aerators have different mass transfer performance characteristics, which contradicts the theoretically expected behavior assessed according to Mersmann. One reason for the higher experimental k_La for the 6 × 0.5 mm open pipe is possibly related to the high protein content of 87 mg/L BSA. The presence of protein is known to decrease the coalescence tendency by stabilizing smaller bubbles by protein adsorption and coverage of the liquid/gas surface (Druzinec, Salzig, Kraume, & Czermak, 2015; Kazakis, Mouza, & Paras, 2008a; Neurath & Bull, 1938; Rosso, Huo, & Stenstrom, 2006; Wagner & Johannes Pöpel, 1996). In consequence, the formation of the resulting bubble size is expected to be highly influenced due to the process of secondary bubble formation and the disintegration of unstable bubbles (Durst & Beer, 1969). In contrast to macrobubbles, stirrer introduced shear forces affect the gas dispersion of microbubbles less, due to their small size (Matthes et al., 2020). In the experimental setup, mixing is provided by a pitch blade turbine with Ne = 1.37 and constant power input of 0.12 W/L. The utilization of a Rushton turbine was avoided due to the possible deactivation of the enzyme by higher local shear forces compared with the Rushton turbine at the employed conditions. In respect to the submerged aeration STR setup, the performance of the macrobubble aeration could be further enhanced by choosing other aerator positions and stirrer types with increased local power input for higher gas dispersion (Bouaifi, Hebrard, Bastoul, & Roustan, 2001; Garcia-Ochoa & Gomez, 2009; Nauha, Visuri, Vermasvuori, & Alopaeus, 2015). The open pipe aeration is indicating a linear behavior between the applied gas stream and a k_La, up to 0.067 vvm, which confirms the literature data (Brierley & Steel, 1959). In contrast to this, the mass transfer performance of the microbubble aeration is increasing as a part of a saturation function until reaching approximately a vvm of one. Considering this behavior, the k_La value is observed to reach a constant value of ~330 ± 10 1/h, when the flow rate is further increased (Figure 3). Reaching the critical flow rate, all pores are activated and the periodic bubble formation region shifts towards the jet gassing region, which occurs when the critical ratio of We^2/Fr reaches above 675 (Mersmann, 1977). To gain a deeper understanding of the observed behavior, investigating the effects of generating bubbles on porous aerator material are of high importance. Khuntia et al. (2012) described the behavior of bubble formation at small pore size aerators, where an increasing aeration rate results in higher capillary pressure and an elevated bubble detachment frequency (Terasaka & Tsuge, 1993). As a result of this, an increased pressure drop at the porous aerator material is initiating the activation of small pores as well as the formation of bubbles over multiple pores at the same time (Kazakis et al., 2008b). Another explanation for this behavior is given by Räbiger et al. (2013) who described a secondary bubble formation occurring over the porous aerator at high gas flows. If the flow rate is increased up to a critical level, the bubble formation over a pore is independent of the flow rate and results in a constant BSD (Mersmann, 1977; Räbiger et al., 2013). Other parameters that affect the BSD and formation of bubbles are the liquid properties, which include surface tension, salt concentration, pH, rheology, and external introduced shear forces (Benedek & Heideger, 1971; Kulkarni & Joshi, 2005). The type of bubble formation over multiple pores correlates with the k_La curve of 1 µm SPG and 2 µm sintered frit, where the flattening of the curve at ~1 vvm indicates the shift to secondary bubble formation. In respect to the described bubble formation behavior, the gas utility is compared at a k_La of 60 1/h and 160 1/h, resulting in applied vvm of 0.05 up to 0.67 for the sintered frit and 1 µm SPG aerator. In contrast to the microbubble aerators, higher gassing rates of 16.67 vvm (5 mm open pipe) and 8.44 vvm (6 × 0.5 mm open pipe) is necessary to achieve a k_La of 160 1/h, which would be uneconomic in process scale-up (Fitschen et al., 2019; Garcia-Ochoa & Gomez, 2009). Nevertheless, both macrobubble aerators are resulting in more reasonable flow rates

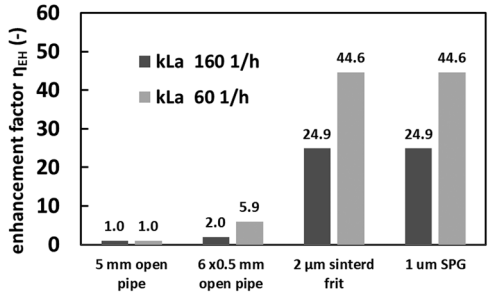

FIGURE 4 Comparison of gas utility enhancement factor of micro- and macrobubble aeration (T = 25°C, V_{medium} = 1000 ml, 10 mM sodium acetate buffer pH 5.3, 87.8 mM D-glucose, 83.3 mg/L BSA, pitched blade turbine at 430 rpm). BSA, bovine serum albumin

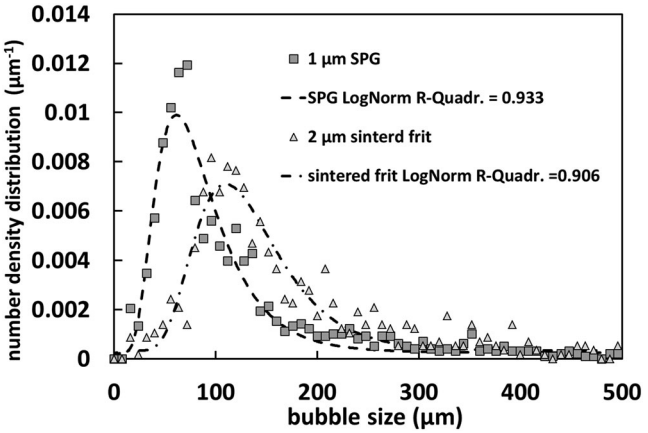

FIGURE 5 Determination of bubble size distribution (BSD) for SPG and sintered frit in GOx containing medium (Sopat probe with a 5-mm gap width, T = 25°C, V_{Medium} = 1000 ml, 10 mM sodium acetate buffer pH 5.3, 83.3 mg/L GOx, pitched blade turbine with 430 rpm, airflow rate of 0.67 vvm). GOx, glucose oxidase; SPG, Shirasu Porous Glass

at a k_La of 60 1/h with 2.23 vvm (5 mm open pipe) and 0.5 vvm (6 × 0.5 mm open pipe). According to Figure 3, an enhancement factor (Equation 4) is calculated for the comparison of the gas utility.

$$\eta_{EH} = \frac{vvm_{sparger}}{vvm_{5mmopenpipe}}, k_La = \text{const} \quad (4)$$

In respect to this, the macrobubble aeration results in 25 times higher gas consumption compared to the microbubble aeration at a k_La of 160 1/h. Comparing the gas utility at k_La of 60 1/h, even lower aeration rates are necessary and the potential for the gas utility of microbubble aeration is even higher (44 times). As mentioned in Figure 4, the gas utility is increasing, if the introduced bubble size is decreasing.

This highlights the high efficiency of fine bubble aeration in view of gas utilization and its enormous potential for the reduction of the gas flow rate. For the application of fine bubbles in the biocatalytic gluconic acid synthesis, an enzyme activity of 11,865 µmol/min (U) is resulting in a high mass transfer limitation. According to Equations 2 and 2, a theoretical k_La value of 5518 1/h is necessary to overcome this mass transfer limitation. To demonstrate the feasibility of microbubble generation in the underlying system with the SPG aerator and sintered frit, the BSD is measured.

The majority of bubbles generated by SPG are in the microbubble region. Compared with the SPG, the bubble generation utilizing the sintered frit is resulting in a higher submillibubble formation. The main difference is the mean pore size of the spargers, which is two times bigger in the case of the sintered frit (2 µm pore size) material. Nevertheless, the BSD of both microbubble aerators shows the occurrence of a high number of bubbles in the microbubble region at the set aeration rate of 0.67 vvm. In respect to the previous k_La measurement, both microbubble aerators are resulting in their average k_La of 160 1/h at a vvm of 0.67. The observed phenomena in microbubble enhanced mass transfer performance are based on three main parameters, which are the increase in volume-specific surface area, residence time, and bubble inner pressure. In this case, the decrease in bubble size towards the microbubble region leads to an increase in the volume-specific interfacial area. For example, a bubble with a diameter d of 100 µm results in a volume-specific area of 6×10^4 m^{-1}, which is 10 folds higher than a macroscopic bubble of d = 1000 µm with 6×10^3 m^{-1}. Most of the bubble generators can produce a defined bubble size distribution that can be adjusted by gassing rate and pressure differences (Terasaka et al., 2011), which applies to the examined microbubble generators. With the assumption of ideal spherical bubbles (φ = 1) and the Sauter mean diameter d_{32} (µm), a specific surface area SV (µm^{-1}) is calculated, described by the Equation (5) (Stieß, 2005).

$$SV = \left(\frac{6 \bullet \varphi}{d_{32}}\right); \dot{a} = SV \bullet \dot{V} \quad (5)$$

For continuous aeration, the theoretical introduced surface area per time $\dot{a}$ (m^2/min) is calculated based on the volumetric aeration rate $\dot{V}$ (m^3/min). For the investigated macrobubble aeration, a form factor of an ellipsoid of 1.77 is assumed. Comparing the introduced surface area $\dot{a}$ at constant k_La of 160 1/h, the microbubble aeration with SPG results in 62.5% lower $\dot{a}$ compared with the aeration with the single hole open pipe (Table 1). The second mass transfer influencing parameter is the residence time of bubbles in the medium. As a result of the decrease in bubble diameter, the rising velocity is decreased, which results in prolonged residence time. Therefore, the bubble interact longer with the surrounding medium. The Stokes law is the classic approach to calculate the theoretical terminal rising velocity of a gas bubble (Parkinson et al., 2008). The assumption of an immobile surface at low Re-numbers Re <<1 is given by the equation of Stokes (Stokes, 1851). The other interpretation (Parkinson et al., 2008) of Naiver-Stokes was done in 1911 by Hadamard and Rybczynsk, which takes the boundary condition, the internal viscosity η (N·s/m^2), and the dispersive phase into account. In respect to the Stokes equation, a microbubble in water, for example, a 10-µm bubble results in a low rising velocity of 0.05 mm/s.

TABLE 1 Comparison of micro- and macrobubble aerators

	1 µm SPG	2 µm sintered frit	5 mm open pipe	6 × 0.5 mm open pipe
d_{av} (mm)	0.118	0.171	8.6[a]	8.6[a]
$d_{3,2}$ (mm)	0.295	0.320	5[a]	5[a]
vvm (l_{air}/min/ l_{Medium})	0.67	0.67	16.67	8.44
k_La (1/h)	160	160	160	160
τ (s)	12.6	10.7	0.044	0.044
$\dot{a}_{Air}$ (m^2/min)	6.667	7.23	10.6	5.36
Δp_{bubble} (kPa)	0.905	0.981	0.057	0.057

Note: Conditions for calculation of Δp and: T = 25°C, η = 0,81 mPas, g = 9.81 m/s^2 ρ_{gas} = 1.18 kg/m^3, ρ_L = 1000 kg/m^3; Kell, 1975; Mersmann, 1977; Straub, Rosner, & Grigull, 1980.

[a]Calculation according to Mersmann correlation.

According to this approach, a small-sized macrobubble with bubble diameter of d_b = 1 mm, is rising with 542.7 mm/s in pure water. Taking the height h (m) of the reactor into account, the resulting residence time τ (s) can be calculated with known gravity constant g (m^3/kg/s^2) as well as the density of gas and liquid ρ (g/m^3) for ideal conditions without stirring.

$$\tau = \frac{d_b^2 \bullet g \bullet (\rho_{Gas} - \rho_{liquid})}{18 \bullet \eta \bullet h} \quad (6)$$

In Table 1, the expected residence times of the bubbles produced by the microbubble (SPG and sintered frit) and the macrobubble (both open pipes) spargers are compared with regard to the achieved Sauter mean diameter. The aeration with the microbubble spargers is beneficial for prolonging the residence time by around 280 times in comparison with macrobubbles (Table 1). The Sauter mean diameter of both open pipe is calculated according to Mersmann to be 5 mm (Mersmann, 1977).

The third influencing parameter is the Young–Laplace pressure within the bubble, which can be calculated with Equation 7.

$$\Delta p_{bubble} = p_b - p_{bulk} = \frac{4 \bullet \sigma}{d_B}; p_b = \frac{c_{O_2}^b}{H} \quad (7)$$

Considering Equation 7, changes in the surface tension σ (N/m) and bubble diameter d_B (m) are directly linked to the pressure difference Δp (Pa). In addition, the pressure inside of the bubble (p_b) is linked via the Henry coefficient H (mol/m^3/Pa) to the concentration $c_{O_2}^b$ (mol/L) in the bubble thin layer (Atkins et al., 2013). Consequently, the shrinking behavior as well as the bubble formation is depending on the surface tension. In a previous study, we reported a decrease of 15.5% in surface tensions of a buffer solution containing 67.8 mg/L BSA or GOx, compared with pure water (Matthes et al., 2020). This change applies to the underlying system. In contrast to this, the variation of the gluconic acid and glucose ratio is resulting in no significant change in surface tension compared with pure water with a measured value of 72.4 mN/m (25°C). Furthermore, the bubble diameter is directly affecting the pressure difference between the inner bubble and the system pressure (Tanaka, Kastens, Fujioka, Schlüter, & Terasaka, 2020). According to Equation 7, the pressure difference is calculated to be 17 times higher, when comparing microbubbles with Sauter mean diameter of 320 µm to macrobubbles with 5 mm (Table 1). The increase in Young–Laplace inner bubble pressure is one of the major reasons for the quick shrinking behavior of fine bubbles. This concentration gradient is the driving force for the diffusion of gas from the bubble into the bulk medium. As reported by Tsuge (2014), microbubbles show quick dissolution amplified by self-compression during the bubble shrinking (Iwakiri et al., 2017). The effect of bubble shrinking is getting more prominent with decreasing bubble size towards a critical diameter of less than 30 µm (Iwakiri et al., 2017; Tanaka et al., 2020).

3.2 | Comparative study of aeration systems on the example of a GOx catalyzed gluconic acid synthesis

To assess the feasibility and gas-saving potential of microbubble aeration in biocatalysis, the productivity of a GOx catalyzed gluconic acid synthesis is investigated. In consequence of the demonstrated high difference in mass transfer performance (Figure 3) and gas utility (Figure 4) between micro- and macrobubble aeration, the simplest 5 mm open pipe is chosen for further comparison. The aerator comparison at constant gassing rate is not chosen, because this results in different k_La values. This in consequence leads to productivity changes according to the different mass transport. On the other hand, the investigation of productivity depending on bubble size with the criteria of constant k_La performance enables the examination of other parameters besides mass transfer performance affecting the productivity of the model reaction. For this comparison, a constant k_La of 160 1/h, according to Figure 3 is adjusted for the aerators. This k_La is chosen to provide the highest measured mass transfer of the 5 mm open pipe and, therefore, the least mass transfer limitation occurring in the system. The chosen k_La

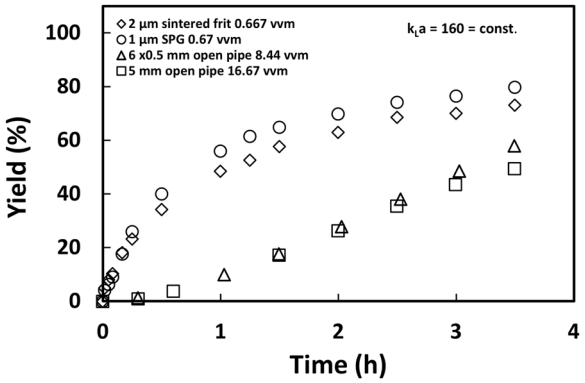

FIGURE 6 Effect of macro- and microbubble aeration on GOx catalyzed reaction. (Conditions: T = 35°C, V = 300 ml in 500 ml glass double-walled reactor, 87.6 mM D-glucose, 11,865 U GOx, 12,320 U Catalase, 10 mM Na-acetate buffer pH = 5.3, pitched blade stirrer at 440 rpm, titration with 0.01 mM KOH in water). GOx, glucose oxidase

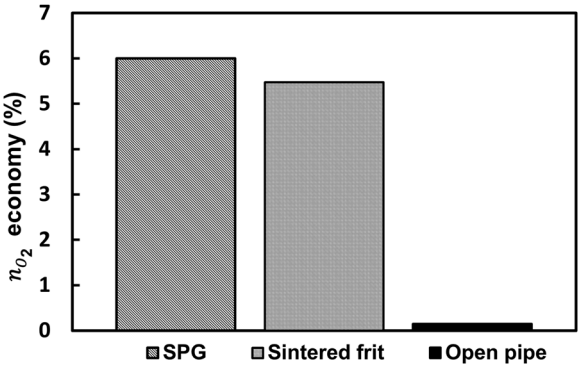

FIGURE 7 Oxygen atom efficiency of the SPG, sintered frit and open pipe aerators applied in GOx catalyzed gluconic acid synthesis. GOx, glucose oxidase; SPG, Shirasu Porous Glass

corresponds to flow rates of 16.67 vvm for the open pipe and 0.67 vvm for the SPG and sintered frit. In the theory of an ideal thermodynamic reaction, identical mass transfer performances will result in identical yield curves, which reach the same equilibrium yield. Yet, different yield curves are measured for the micro- and macrobubble spargers, as shown in Figure 6. For quantification and comparison, an operative time efficiency factor η_{op} is introduced. This factor is defined as the ratio of reaction time, which is necessary to reach 50% analytical yield for the open pipe and sintered frit related to the SPG experiment (Equation (8).

$$\eta_{op} = \frac{t_{Y=50\%,\text{aerator}}}{t_{Y=50\%,\text{SPG}}} \tag{8}$$

The gluconic acid synthesis with the SPG aerator is determined to be 4.58 times faster compared with open pipe aeration. Compared with the sintered frit aeration, the reaction is with an enhancement of 1.2 slightly faster under the investigated conditions. However, taking the deviation of ±10% in k_La adjustment as well as the nearly similar BSD (Figure 5) into account, the SPG and sintered frit give comparable results under the investigated reaction conditions. For a different interpretation of the aerator results, the productivity after a reaction time of 3.5 h is compared. After 3.5 h, sodium gluconate productivities of 21.35 g/L with SPG, 19.59 g/L with sintered frit and 12.78 g/L with open pipe aeration are achieved (Figure 6). Considering that only the aerator systems are varied, the difference between micro- and macrobubbles should be related to the aeration coupled effects. Especially, the difference in up to 16 vvm gassing rate between micro- and macrobubble aeration in the system is one factor to cause the yield deviation. The gassing rate influences the interaction between enzyme and gas-liquid interface as well as introduced shear forces, which could cause enzyme deactivation (Bhagia, Dhir, Kumar, & Wyman, 2018; D'Imprima et al., 2019).

Overall, a significant improvement in productivity by application of microbubble in comparison to macrobubble aeration is achieved. Furthermore, microbubble aeration improves the gas utilization, which is compared by the atom balance of oxygen applied to the reaction medium related to the bound oxygen during the biotransformation. Therefore, in Equation 9, the oxygen atoms bound in the product gluconic acid ($n_{\text{gluconic acid}}/2$) per reaction time are normalized to the molar stream of oxygen, which was introduced by the airflow rate into the system ($t \bullet \dot{n}_{O_2,\text{total}}$).

$$n_{O_2\text{economy}}[\%] = \frac{n_{\text{gluconicacid}}}{2 \bullet t \bullet \dot{n}_{O_2,\text{total}}} \tag{9}$$

As demonstrated in Figure 7, the fixation of oxygen atoms in the reaction product by applying microbubble aeration through SPG and sintered frit is enhanced by factors of 41.6 and 38 compared with the open pipe aeration, respectively. The total atom economy of microbubble aeration is 6% for SPG and 5.6% for sintered frit making this an efficient aeration system. In contrast, 0.14% of the introduced oxygen is bound in the product gluconic acid with applied macrobubble aeration.

This further highlights the improvement when using microbubble aeration. Reasons for the resulting lower oxygen atom economy of the macrobubble aeration are possible deactivation of the enzyme. Enzymes are known to deactivate in the presence of a second phase as it is reported for several enzymes (Bhagia et al., 2018; Bommarius & Karau, 2005; D'Imprima et al., 2019). Furthermore, oxidation of enzymes by dissolved oxygen could cause additional deactivation. Additional to the shear forces introduced by stirring, coalescence, bubble break up as well as foam formation adds shear forces. In the experiments, less foam formation is observed during microbubble aeration. Therefore, the difference in atom economy and productivity is likely related to the denaturation of the enzymes as a result of interacting with the interfacial area (D'Imprima et al., 2019). The exact mechanism to cause the productivity difference in view of GOx stability needs further investigation. Nevertheless, the underlying study is giving a first approximation of the benefits of applying microbubbles in a stirred tank setup. Microbubble aeration is found to improve the mass transport, operative time efficiency

factor, and gas utilization. These identified benefits are promising for optimization of biocatalytic and chemical reactions in multiphase systems, which are limited by the low solubility of the gaseous substrate or gas in general.

4 | CONCLUSIONS

This study focuses on the comparative investigation of microbubble and macrobubble aeration applied in oxygen-consuming GOx catalyzed biotransformation towards the product gluconic acid. The GOx Type VII is identified as a suitable catalyst with high activity, suitable reaction conditions, and sufficient storage stability, which enables mass transfer limitation conditions for the investigation of different aerator types. The investigation shows that the microbubble aerators, SPG and sintered frit, achieve significantly higher mass transport performance in the vvm range of 0.017–16.67 compared with open pipe macrobubble aeration in a BSA containing solution. The application of microbubbles in a β-D-glucose consuming enzymatic model reaction is resulting in a 32% higher yield (after 3.5 h). This is coupled with a 25-fold higher gas utility (at constant k_La of 160 1/h) compared with macrobubble aeration. The atom economy of the overall introduced oxygen is calculated to be 6% for the SPG aerator, 5.6% for the sintered frit, and 0.14% for the open pipe. Due to this, the oxygen economy of SPG and sintered frit aeration is enhanced by the factor of 41.6 and 38 compared with the open pipe aeration, respectively. Thus, the application of microbubbles is shown to be beneficial in view of yield, gas utility, oxygen atom economy, and mass transfer performance in general. Especially, the enhanced gas utilization provides high potential in cost reduction and should be applied in the optimization of processes, which are limited by the low solubility of the gaseous substrate.

This is offering the possibility to reduce the production costs by saving gas and reducing off-gas streams in industrial biocatalysis and chemical applications.

ACKNOWLEDGMENTS

We are grateful for the financial support provided by the Deutsche Forschungsgemeinschaft (DFG) within the combined project LI 899/10-1 and SCHL 617/14-1. We want to thank the lab apprentices Friederike Dellien, Marie Gruber, Mary Huynh, and Huyen Vu for their excellent help in the laboratory. Open access funding enabled and organized by Projekt DEAL.

AUTHOR CONTRIBUTIONS

Benjamin Thomas designed and performed the experiments. Benjamin Thomas wrote the manuscript with support from Daniel Ohde, Simon Matthes, Claudia Engelmann, Paul Bubenheim, Koichi Terasaka, Michael Schlüter, and Andreas Liese. Koichi Terasaka, Michael Schlüter, and Andreas Liese directed and supervised the project. All authors discussed the results and contributed to the final manuscript.

ORCID

Benjamin Thomas https://orcid.org/0000-0002-6416-5440
Daniel Ohde https://orcid.org/0000-0002-5482-3534
Simon Matthes https://orcid.org/0000-0002-3123-6521
Claudia Engelmann https://orcid.org/0000-0003-0376-8122
Paul Bubenheim https://orcid.org/0000-0001-6954-4274
Koichi Terasaka https://orcid.org/0000-0002-9978-5463
Michael Schlüter https://orcid.org/0000-0001-5969-2150
Andreas Liese http://orcid.org/0000-0002-4867-9935

REFERENCES

Atkins, P. W., de Paula, J, & Michael, B. (2013). *Physikalische Chemie. Wiley VCH Lehrbuchkollektion 1 (5 Auf)*. Weinheim, Germany: Wiley-VCH. https://doi.org/10.1002/3527682899

Bankar, S. B., Bule, M. V., Singhal, R. S., & Ananthanarayan, L. (2009). Glucose oxidase—an overview. *Biotechnology Advances*, *27*(4), 489–501. https://doi.org/10.1016/j.biotechadv.2009.04.003

Bao, J., Furumoto, K., Yoshimoto, M., Fukunaga, K., & Nakao, K. (2003). Competitive inhibition by hydrogen peroxide produced in glucose oxidation catalyzed by glucose oxidase. *Biochemical Engineering Journal*, *13*(1), 69–72. https://doi.org/10.1016/S1369-703X(02)00120-1

Bateman, R. C., & Evans, J. A. (1995). Using the glucose oxidase/peroxidase system in enzyme kinetics. *Journal of Chemical Education*, *72*(12), A240. https://doi.org/10.1021/ed072pA240

Benedek, A., & Heideger, W. J. (1971). Effect of additives on mass transfer in turbine aeration. *Biotechnology and Bioengineering*, *13*(5), 663–684. https://doi.org/10.1002/bit.260130507

Bhagia, S., Dhir, R., Kumar, R., & Wyman, C. E. (2018). Deactivation of cellulase at the air-liquid interface is the main cause of incomplete cellulose conversion at low enzyme loadings. *Scientific Reports*, *8*(1), 1350. https://doi.org/10.1038/s41598-018-19848-3

Bolivar, J. M., Mannsberger, A., Thomsen, M. S., Tekautz, G., & Nidetzky, B. (2019). Process intensification for O_2 -dependent enzymatic transformations in continuous single-phase pressurized flow. *Biotechnology and Bioengineering*, *116*(3), 503–514. https://doi.org/10.1002/bit.26886

Bommarius, A. S., & Karau, A. (2005). Deactivation of formate dehydrogenase (FDH) in solution and at gas-liquid interfaces. *Biotechnology Progress*, *21*(6), 1663–1672. https://doi.org/10.1021/bp050249q

Bouaifi, M., Hebrard, G., Bastoul, D., & Roustan, M. (2001). A comparative study of gas hold-up, bubble size, interfacial area and mass transfer coefficients in stirred gas–liquid reactors and bubble columns. *Chemical Engineering and Processing: Process Intensification*, *40*(2), 97–111. https://doi.org/10.1016/S0255-2701(00)00129-X

Brierley, M. R., & Steel, R. (1959). Agitation-aeration in submerged fermentation: II. Effect of solid disperse phase on oxygen absorption in a fermentor. *Applied Microbiology*, *7*(1), 57–61.

Chapman, M. R., Cosgrove, S. C., Turner, N. J., Kapur, N., & Blacker, A. J. (2018). Highly productive oxidative biocatalysis in continuous flow by enhancing the aqueous equilibrium solubility of oxygen. *Angewandte Chemie (International Ed. In English)*, *57*(33), 10535–10539. https://doi.org/10.1002/anie.201803675

Collins, G. L., Motarjemi, M., & Jameson, G. J. (1978). A method for measuring the charge on small gas bubbles. *Journal of Colloid and Interface Science*, *63*(1), 69–75. https://doi.org/10.1016/0021-9797(78)90036-X

Di Wang, Yang, X., Tian, C., … Zhang, Z. (2019). Characteristics of ultrafine bubble water and its trials on enhanced methane production from waste activated sludge. *Bioresource Technology*, *273*, 63–69. https://doi.org/10.1016/j.biortech.2018.10.077

D'Imprima, E., Floris, D., Joppe, M., Sánchez, R., Grininger, M., & Kühlbrandt, W. (2019). Protein denaturation at the air-water interface and how to prevent it. *eLife*, 8. https://doi.org/10.7554/eLife.42747

Druzinec, D., Salzig, D., Kraume, M., & Czermak, P. (2015). Micro-bubble aeration in turbulent stirred bioreactors: Coalescence behavior in Pluronic F68 containing cell culture media. *Chemical Engineering Science*, *126*, 160–168. https://doi.org/10.1016/j.ces.2014.12.020

Durst, F., & Beer, H. (1969). Blasenbildung an düsen bei gasdispersionen in flüssigkeiten. *Chemie Ingenieur Technik*, *41*(18), 1000–1006. https://doi.org/10.1002/cite.330411803

Duval, E., Adichtchev, S., Sirotkin, S., & Mermet, A. (2012). Long-lived submicrometric bubbles in very diluted alkali halide water solutions. *Physical Chemistry Chemical Physics*, *14*(12), 4125–4132. https://doi.org/10.1039/c2cp22858k

Epstein, P. S., & Plesset, M. S. (1950). On the stability of gas bubbles in liquid-gas solutions. *The Journal of Chemical Physics*, *18*(11), 1505–1509. https://doi.org/10.1063/1.1747520

Fitschen, J., Maly, M., Rosseburg, A., Wutz, J., Wucherpfennig, T., & Schlüter, M. (2019). Influence of spacing of multiple impellers on power input in an industrial-scale aerated stirred tank reactor. *Chemie Ingenieur Technik*, *91*(12), 1794–1801. https://doi.org/10.1002/cite.201900121

Gaddis, E. S. (2013). *N3 Wärmeübertragung und Leistungsaufnahme in Rührkesseln. In* VDI-Buch. VDI-Wärmeatlas: Mit 320 Tabellen (11th ed., 51, pp. 1621–1654). Berlin, Germany: Springer Vieweg. https://doi.org/10.1007/978-3-642-19981-3_108

Garcia-Ochoa, F., & Gomez, E. (2009). Bioreactor scale-up and oxygen transfer rate in microbial processes: An overview. *Biotechnology Advances*, *27*(2), 153–176. https://doi.org/10.1016/j.biotechadv.2008.10.006

Gemoets, H. P. L., Hessel, V., & Noël, T. (2016). Reactor concepts for aerobic liquid phase oxidation: Microreactors and tube reactors. In S. S. Stahl & P. L. Alsters (Eds.), *Liquid phase aerobic oxidation catalysis: Industrial applications and academic perspectives* (45, pp. 397–419). Weinheim, Germany: Wiley-VCH Verlag GmbH & Co. KGaA. https://doi.org/10.1002/9783527690121.ch23

Guy, C., Carreau, P. J., & Paris, J. (1986). Mixing characteristics and gas hold-up of a bubble column. *The Canadian Journal of Chemical Engineering*, *64*(1), 23–35. https://doi.org/10.1002/cjce.5450640104

Hernandez, K., Berenguer-Murcia, A., C. Rodrigues, R., & Fernandez-Lafuente, R. (2012). Hydrogen peroxide in biocatalysis. A dangerous liaison. *Current Organic Chemistry*, *16*(22), 2652–2672. https://doi.org/10.2174/138527212804004526

Hone, C. A., & Kappe, C. O. (2018). The use of molecular oxygen for liquid phase aerobic oxidations in continuous flow. *Topics in Current Chemistry*, *377*(1), 2. https://doi.org/10.1007/s41061-018-0226-z

Huo, W., Zhang, X., Gan, K., Chen, Y., Xu, J., & Yang, J. (2019). Effect of zeta potential on properties of foamed colloidal suspension. *Journal of the European Ceramic Society*, *39*(2-3), 574–583. https://doi.org/10.1016/j.jeurceramsoc.2018.08.035

Iwakiri, M., Terasaka, K., Fujioka, S., Schluter, M., Kastens, S., & Tanaka, S. (2017). Mass Transfer from a shrinking single microbubble rising in water. *Japanese Journal of Multiphase Flow*, *30*(5), 529-535. https://doi.org/10.3811/jjmf.30.529

Jia, H., Xiao, X., & Kang, Y. (2019). Investigation of a free rising bubble with mass transfer by an arbitrary Lagrangian–Eulerian method. *International Journal of Heat and Mass Transfer*, *137*, 545–557. https://doi.org/10.1016/j.ijheatmasstransfer.2019.03.117

Kaufhold, D., Kopf, F., Wolff, C., Beutel, S., Hilterhaus, L., Hoffmann, M., … Liese, A. (2012). Generation of Dean vortices and enhancement of oxygen transfer rates in membrane contactors for different hollow fiber geometries. *Journal of Membrane Science*, *423-424*, 342–347. https://doi.org/10.1016/j.memsci.2012.08.035

Kazakis, N. A., Mouza, A. A., & Paras, S. V. (2008a). Coalescence during bubble formation at two neighbouring pores: An experimental study in microscopic scale. *Chemical Engineering Science*, *63*(21), 5160–5178. https://doi.org/10.1016/j.ces.2008.07.006

Kazakis, N. A., Mouza, A. A., & Paras, S. V. (2008b). Experimental study of bubble formation at metal porous spargers: Effect of liquid properties and sparger characteristics on the initial bubble size distribution. *Chemical Engineering Journal*, *137*(2), 265–281. https://doi.org/10.1016/j.cej.2007.04.040

Kell, G. S. (1975). Density, thermal expansivity, and compressibility of liquid water from 0.deg. to 150.deg. Correlations and tables for atmospheric pressure and saturation reviewed and expressed on 1968 temperature scale. *Journal of Chemical & Engineering Data*, *20*(1), 97–105. https://doi.org/10.1021/je60064a005

Khuntia, S., Majumder, S. K., & Ghosh, P. (2012). Microbubble-aided water and wastewater purification: A review. *Reviews in Chemical Engineering*, *28*(4-6). https://doi.org/10.1515/revce-2012-0007

Kulkarni, A. A., & Joshi, J. B. (2005). Bubble formation and bubble rise velocity in gas−liquid systems: A review. *Industrial & Engineering Chemistry Research*, *44*(16), 5873–5931. https://doi.org/10.1021/ie049131p

Lee (2020). Baseline mass-transfer coefficient and interpretation of nonsteady state submerged bubble-oxygen transfer data. *Journal of Environmental Engineering*, *146*(1), 4019102. https://doi.org/10.1061/(ASCE)EE.1943-7870.0001624

Leung, R., Poncelet, D., & Neufeld, R. J. (1997). Enhancement of oxygen transfer rate using microencapsulated silicone oils as oxygen carriers. *Journal of Chemical Technology & Biotechnology*, *68*(1), 37–46. https://doi.org/10.1002/(SICI)1097-4660(199701)68:1<37::AID-JCTB601>3.0.CO;2-Y

Lindeque, R. M., & Woodley, J. M. (2020), acs.oprd.0c00140. The effect of dissolved oxygen on kinetics during continuous biocatalytic oxidations. *Organic Process Research & Development*. Advance online publication. https://doi.org/10.1021/acs.oprd.0c00140

Liu, B., Xiao, Q., Sun, N., Gao, P., Fan, F., & Sunden, B. (2019). Effect of gas distributor on gas–liquid dispersion and mass transfer characteristics in stirred tank. *Chemical Engineering Research and Design*, *145*, 314–322. https://doi.org/10.1016/j.cherd.2019.03.035

Liu, X., T.-M., Zhang., Zhang, L., Yang, J.-L., & Zhang, M. (2014). Effect of membrane wettability on membrane fouling and chemical durability of SPG membranes used in a microbubble-aerated biofilm reactor. *Separation and Purification Technology*, *127*, 157–164. https://doi.org/10.1016/j.seppur.2014.03.001

Ludwig, H., & Macdonald, A. G. (2005). The significance of the activity of dissolved oxygen, and other gases, enhanced by high hydrostatic pressure. *Comparative Biochemistry and Physiology Part A: Molecular & Integrative Physiology*, *140*(4), 387–395. https://doi.org/10.1016/j.cbpb.2005.02.001

Mafra, A. C. O., Furlan, F. F., Badino, A. C., & Tardioli, P. W. (2015). Gluconic acid production from sucrose in an airlift reactor using a multi-enzyme system. *Bioprocess and Biosystems Engineering*, *38*(4), 671–680. https://doi.org/10.1007/s00449-014-1306-2

Matthes, S., Thomas, B., Ohde, D., Hoffmann, M., Bubenheim, P., Liese, A., … Schlüter, M. (2020). Hydrodynamic and Mass Transfer Correlation in a Microbubble Aerated Stirred Tank Reactor. *Journal of Chemical Engineering of Japan*. Accepted manuscript.

Mersmann, A. (1977). Auslegung und Maßstabsvergrößerung von Blasen- und Tropfensäulen. *Chemie Ingenieur Technik*, *49*(9), 679–691. https://doi.org/10.1002/cite.330490902

Nakamura, S., Hayashi, S., & Koga, K. (1976). Effect of periodate oxidation on the structure and properties of glucose oxidase. *Biochimica Et Biophysica Acta (BBA) - Enzymology*, *445*(2), 294–308. https://doi.org/10.1016/0005-2744(76)90084-X

Nauha, E. K., Visuri, O., Vermasvuori, R., & Alopaeus, V. (2015). A new simple approach for the scale-up of aerated stirred tanks. *Chemical Engineering Research and Design*, *95*, 150–161. https://doi.org/10.1016/j.cherd.2014.10.015

Neurath, H., & Bull, H. B. (1938). The surface activity of proteins. *Chemical Reviews*, *23*(3), 391–435. https://doi.org/10.1021/cr60076a001

Oliveira, C., & Rubio, J. (2011). Zeta potential of single and polymer-coated microbubbles using an adapted microelectrophoresis technique. *International Journal of Mineral Processing*, *98*(1), 118–123. https://doi.org/10.1016/j.minpro.2010.10.006

Parkinson, L., Sedev, R., Fornasiero, D., & Ralston, J. (2008). The terminal rise velocity of 10-100 microm diameter bubbles in water. *Journal of Colloid and Interface Science*, *322*(1), 168–172. https://doi.org/10.1016/j.jcis.2008.02.072

Räbiger, N., Schlüter, M., Mersmann, A., Dahl, H. D., Luke, A., Walzel, P., & Musemic, E. (2013). L4 Blasen und Tropfen in technischen apparaten, *VDI-Buch. VDI-Wärmeatlas: Mit 320 Tabellen* (11th ed., pp. 1413–1458). Berlin, Germany: Springer Vieweg. https://doi.org/10.1007/978-3-642-19981-3_92

Rissom, S., Schwarz-Linek, U., Vogel, M., Tishkov, V. I., & Kragl, U. (1997). Synthesis of chiral ε-lactones in a two-enzyme system of cyclohexanone mono-oxygenase and formate dehydrogenase with integrated bubble-free aeration. *Tetrahedron: Asymmetry*, *8*(15), 2523–2526. https://doi.org/10.1016/S0957-4166(97)00311-X

Romero, E., Gómez Castellanos, J. R., Gadda, G., Fraaije, M. W., & Mattevi, A. (2018). Same substrate, many reactions: oxygen activation in flavoenzymes. *Chemical Reviews*, *118*(4), 1742–1769. https://doi.org/10.1021/acs.chemrev.7b00650

Rosso, D., Huo, D. L., & Stenstrom, M. K. (2006). Effects of interfacial surfactant contamination on bubble gas transfer. *Chemical Engineering Science*, *61*(16), 5500–5514. https://doi.org/10.1016/j.ces.2006.04.018

Silva, A. R. D., Tomotani, E. J., & Vitolo, M. (2011). Invertase, glucose oxidase and catalase for converting sucrose to fructose and gluconic acid through batch and membrane-continuous reactors. *Brazilian Journal of Pharmaceutical Sciences*, *47*(2), 399–407. https://doi.org/10.1590/S1984-82502011000200022

Stieß, M. (2005). *Mechanische Verfahrenstechnik (2. Aufl.)*. Berlin, Heidelberg, New York: Springer.

Stokes, G. G. (1851). On the effect of the internal friction of fluids on the motion of pendulums (Vol. 9, p. 8). Cambridge, UK: Pitt Press.

Straub, J., Rosner, N., & Grigull, U. (1980). Oberflächenspannung von leichtem und schwerem Wasser. *Wärme - Und Stoffübertragung*, *13*(4), 241–252. https://doi.org/10.1007/BF01002412

Struthwolf, M., & Blanchard, D. C. (1984). The residence time of air bubbles <400 μm diameter at the surface of distilled water and seawater. *Tellus B: Chemical and Physical Meteorology*, *36*(4), 294–299. https://doi.org/10.3402/tellusb.v36i4.14911

Tanaka, S., Kastens, S., Fujioka, S., Schlüter, M., & Terasaka, K. (2020). Mass transfer from freely rising microbubbles in aqueous solutions of surfactant or salt. *Chemical Engineering Journal*, *387*, 121246. https://doi.org/10.1016/j.cej.2019.03.122

Tao, D. (2005). Role of bubble size in flotation of coarse and fine particles—A review. *Separation Science and Technology*, *39*(4), 741–760. https://doi.org/10.1081/SS-120028444

Temesgen, T., Bui, T. T., Han, M., Kim, T.-I., & Park, H. (2017). Micro and nanobubble technologies as a new horizon for water-treatment techniques: A review. *Advances in Colloid and Interface Science*, *246*, 40–51. https://doi.org/10.1016/j.cis.2017.06.011

Terasaka, K., Hirabayashi, Ai, Nishino, T., Fujioka, S., & Kobayashi, D. (2011). Development of microbubble aerator for waste water treatment using aerobic activated sludge. *Chemical Engineering Science*, *66*(14), 3172–3179. https://doi.org/10.1016/j.ces.2011.02.043

Terasaka, K., & Tsuge, H. (1993). Bubble formation under constant-flow conditions. *Chemical Engineering Science*, *48*(19), 3417–3422. https://doi.org/10.1016/0009-2509(93)80159-N

Toftgaard Pedersen, A., de Carvalho, T. M., Sutherland, E., Rehn, G., Ashe, R., & Woodley, J. M. (2017). Characterization of a continuous agitated cell reactor for oxygen dependent biocatalysis. *Biotechnology and Bioengineering*, *114*(6), 1222–1230. https://doi.org/10.1002/bit.26267

Tomotani, E. J., das Neves, L. C. M., & Vitolo, M. (2005). Oxidation of glucose to gluconic acid by glucose oxidase in a membrane bioreactor. *Applied Biochemistry and Biotechnology*, *121*(1-3), 149–162. https://doi.org/10.1385/ABAB:121:1-3:0149

Tribe, L. A., Briens, C. L., & Margaritis, A. (1995). Determination of the volumetric mass transfer coefficient (k(L)a) using the dynamic "gas out-gas in" method: Analysis of errors caused by dissolved oxygen probes. *Biotechnology and Bioengineering*, *46*(4), 388–392. https://doi.org/10.1002/bit.260460412

Tsuge (Ed.) (2014). *Micro- and nanobubbles: Fundamentals and applications*. Singapore: Pan Stanford Publishing.

Tsuge, H., & Hibino, S.-I. (1983). Bubble formation from an orifice submerged in liquids. *Chemical Engineering Communications*, *22*(1-2), 63–79. https://doi.org/10.1080/00986448308940046

Ushikubo, F. Y., Enari, M., Furukawa, T., Nakagawa, R., Makino, Y., Kawagoe, Y., & Oshita, S. (2010). Zeta-potential of micro- and/or nano-bubbles in water produced by some kinds of gases. *IFAC Proceedings Volumes*, *43*(26), 283–288. https://doi.org/10.3182/20101206-3-jp-3009.00050

Wagner, M., & Johannes Pöpel, H. (1996). Surface active agents and their influence on oxygen transfer: Water Quality International '96 Part 2. *Water Science and Technology*, *34*(3), 249–256. https://doi.org/10.1016/0273-1223(96)00580-X

Wang, L., Wang, Y., Yan, X., Wang, A., & Cao, Y. (2017). A numerical study on efficient recovery of fine-grained minerals with vortex generators in pipe flow unit of a cyclonic-static micro bubble flotation column. *Chemical Engineering Science*, *158*, 304–313. https://doi.org/10.1016/j.ces.2016.10.037

Weiss, R. F. (1970). The solubility of nitrogen, oxygen and argon in water and seawater. *Deep Sea Research and Oceanographic Abstracts*, *17*(4), 721–735. https://doi.org/10.1016/0011-7471(70)90037-9

Wilson, R., & Turner, A. P. F. (1992). Glucose oxidase: An ideal enzyme. *Biosensors and Bioelectronics*, *7*(3), 165–185. https://doi.org/10.1016/0956-5663(92)87013-F

Woodley, J. M. (2019). Reaction engineering for the industrial implementation of biocatalysis. *Topics in Catalysis*, *62*(17-20), 1202–1207. https://doi.org/10.1007/s11244-019-01154-5

Xing, W., Yin, M., Lv, Q., Hu, Y., Liu, C., & Zhang, J. (2014). Oxygen solubility, diffusion coefficient, and solution viscosity. In W. Xing, G. Yin, & J. Zhang (Eds.), *Rotating electrode methods and oxygen reduction electrocatalysts* (pp. 1–31). Amsterdam, The Netherlands: Elsevier. https://doi.org/10.1016/B978-0-444-63278-4.00001-X

Zhai, J., Li, H., Wong, A. H.-H., Dong, C., Yi, S., Jia, Y., … Martins, R. P. (2020). A digital microfluidic system with 3D microstructures for single-cell culture. *Microsystems & Nanoengineering*, *6*(1), 381. https://doi.org/10.1038/s41378-019-0109-7

Zhang, P., Sun, D., Cho, A., Weon, S., Lee, S., Lee, J., … Choi, W. (2019). Modified carbon nitride nanozyme as bifunctional glucose oxidase-peroxidase for metal-free bioinspired cascade photocatalysis. *Nature Communications*, *10*(1), 940. https://doi.org/10.1038/s41467-019-08731-y

How to cite this article: Thomas B, Ohde D, Matthes S, et al. Comparative investigation of fine bubble and macrobubble aeration on gas utility and biotransformation productivity. *Biotechnology and Bioengineering*. 2021;118:130–141. https://doi.org/10.1002/bit.27556